M&C 2017 - International Conference on Mathematics & Computational Methods Applied to Nuclear Science & Engineering, Jeju, Korea, April 16-20, 2017, on USB (2017)

An Adapted Cross Section Collapsing Method For Few-Group SP_n Calculations

Ansar Calloo and David Couyras

EDF R&D
7, boulevard Gaspard Monge, 91 120 Palaiseau, France
ansar.calloo@edf.fr, david.couyras@edf.fr

Abstract - *EDF R&D is currently working on a new, state-of-the-art calculation chain called ANDROMÈDE. For core computations, it uses the 3D Cartesian code,* Cocagne. Cocagne *is a platform which provides several engineering solutions as well as advanced solutions such as several solvers based on the SP_n (diffusion is a particular case of SP_1 equations) and S_n methods for the time-independent Boltzmann equation.* Cocagne *is fed with condensed and homogenised cross sections generated in the assembly calculation. In the present state, the homogenisation-condensation process is carried out using the scalar flux. The latter may not be well suited to produce cross sections for highly heterogeneous problems. The goal of this paper is to define a simple method to condense cross section using an approximate for the first flux moment. The method is then tested on assembly clusters with UOX-MOX interfaces and a numerical benchmark case called the KAIST 1A benchmark.*

I. INTRODUCTION

The time-independent Boltzmann transport equation describes the statistical behaviour of a population of neutral particles in a system at equilibrium. Basically, it is a balance equation between particles which are removed from and added to a given control volume (streaming term), those which disappear by absorption and scattering and those produced in the control volume (source term). It is one of the most used equations in reactor physics under a given set of assumptions [1] and its numerical resolution to obtain the neutron flux is widely applied for computations regarding the industrial monitoring of existing nuclear reactors and for the design of future systems.

EDF R&D is working on a state-of-the-art calculation chain called *ANDROMÈDE*. The latter encompasses the Apollo2 code/JEFF3-based CEA multigroup library/REL2005 scheme package for assembly computations to generate few-group cross sections for the 3D code Cocagne for core computations. *ANDROMÈDE* has the advantage of providing industrial two-group diffusion approximation for everyday uses by operational teams as well as multigroup transport schemes for advanced engineering and R&D purposes.

This paper focuses on the solution of the Boltzmann equation using the *Simplified P_n* method within the Cocagne framework. Past results [2, 3] obtained on the KAIST benchmark [4] with the SP_n method have shown that below 8 energy groups, the SP_n method does not give satisfactory results on the benchmark. Indeed, few-group cross sections are not appropriate to deal with problems that require spectrally rich data (*e.g.* UOX-MOX interface, core-reflector interface). The goal of this paper is to provide a method to generate few-group cross sections that are suitable for such problems.

The first section presents the theoretical background surrounding cross section condensation and the method which has been applied in this work. Afterwards, we describe the results applied to assembly clusters with UOX-MOX interfaces and the KAIST 1A benchmark. The results will be compared to reference calculations, and will be discussed.

II. THEORY

1. Energy collapsing for multigroup cross sections

Cross sections provided to the core code are obtained via an energy condensation with a weighting function. Consider the following multigroup Boltzmann equation, with N_g energy groups:

$$\mathbf{\Omega}.\nabla\phi^g(\mathbf{r},\mathbf{\Omega}) + \Sigma_t^g(\mathbf{r})\phi^g(\mathbf{r},\mathbf{\Omega}) = \frac{1}{2\pi}\sum_{l=0}^{L}\frac{2l+1}{2}\sum_{g=1}^{N_g}\Sigma_{sl}^{g'\to g}(\mathbf{r})\sum_{m=-l}^{l}\phi_l^{m,g'}(\mathbf{r})R_l^m(\mathbf{\Omega}) + q^g(\mathbf{r},\mathbf{\Omega}) \tag{1}$$

with

- $\mathbf{\Omega}.\nabla\phi^g(\mathbf{r},\mathbf{\Omega})$: streaming term for particles entering or going out of the control volume
- $\Sigma_t^g(\mathbf{r})\phi^g(\mathbf{r},\mathbf{\Omega})$: total reaction rate within the control volume
- $\frac{1}{2\pi}\sum_{l=0}^{L}\frac{2l+1}{2}\sum_{g=1}^{N_g}\Sigma_{sl}^{g'\to g}(\mathbf{r})\sum_{m=-l}^{l}\phi_l^{m,g'}(\mathbf{r})R_l^m(\mathbf{\Omega})$: scattering source
- $q^g(\mathbf{r},\mathbf{\Omega})$: production source in the control volume (*e.g.* by fission)

The energy collapsing from N_g energy groups to N_G energy groups of the multigroup neutron transport equation is expressed by summing over the micro-groups g which belong to each coarse group G, and the resulting equation is

$$\mathbf{\Omega}.\nabla\phi^G(\mathbf{r},\mathbf{\Omega}) + \Sigma_t^G(\mathbf{r},\mathbf{\Omega})\phi^G(\mathbf{r},\mathbf{\Omega}) = \frac{1}{2\pi}\sum_{l=0}^{L}\frac{2l+1}{2}\sum_{G=1}^{N_G}\Sigma_{sl}^{m,G'\to G}(\mathbf{r})\sum_{m=-l}^{l}\phi_l^{m,G'}(\mathbf{r})R_l^m(\mathbf{\Omega}) + q^G(\mathbf{r},\mathbf{\Omega}) \tag{2}$$

with:

$$\phi^G(\mathbf{r},\mathbf{\Omega}) = \sum_{g\in G}\phi^g(\mathbf{r},\mathbf{\Omega})$$

$$\Sigma_t^G(\mathbf{r},\mathbf{\Omega}) = \frac{\sum_{g\in G}\Sigma_t^g(\mathbf{r})\phi^g(\mathbf{r},\mathbf{\Omega})}{\sum_{g\in G}\phi^g(\mathbf{r},\mathbf{\Omega})}$$

$$\Sigma_{sl}^{m,G'\to G}(\mathbf{r}) = \frac{\sum_{g'\in G'}\sum_{g\in G}\Sigma_{sl}^{g'\to g}(\mathbf{r})\phi_l^{m,g'}(\mathbf{r})}{\sum_{g'\in G'}\phi_l^{m,g'}(\mathbf{r})}$$

Thus, the weighting function for the cross section should strictly be an angular flux. It should be noted that in this case, the total cross section and the differential scattering cross section have an angular dependence and requires modification of the solvers to deal with such equations or employing the method given in [5]. However, given that the angular flux is seldom available from codes such as Apollo2, the scalar flux is used as an approximation as the weighting function:

$$\Sigma_t^G(\mathbf{r}) = \frac{\sum_{g\in G}\Sigma_t^g(\mathbf{r})\phi_0^g(\mathbf{r})}{\sum_{g\in G}\phi_0^g(\mathbf{r})} \tag{3}$$

$$\Sigma_{sl}^{G'\to G}(\mathbf{r}) = \frac{\sum_{g'\in G'}\sum_{g\in G}\Sigma_{sl}^{g'\to g}(\mathbf{r})\phi_0^{g'}(\mathbf{r})}{\sum_{g'\in G'}\phi_0^{g'}(\mathbf{r})} \tag{4}$$

where $\phi_0^g(\mathbf{r})$ is the scalar flux defined as:

$$\phi_0^g(\mathbf{r}) = \int_{4\pi} \mathrm{d}^2\mathbf{\Omega}\ \phi^g(\mathbf{r},\mathbf{\Omega}) \tag{5}$$

Nonetheless, such weighting means that angular data is lost during condensation as has been shown by [5]. In *ANDROMÈDE*, given that the Apollo2-REL2005 calculations are carried out at 26 energy groups, cross sections for Cocagne can be generated by weighting with the scalar flux for 2 to 26 energy groups. However, as was shown with the past works [2, 3], few groups cross sections cannot deal with the highly heterogeneous interfaces such as the core-reflector interface. A more appropriate method would be an energy condensation by the flux moments, but these are not readily available to the user from our lattice code Apollo2.

2. SP_n equations

The *Simplified* P_n or SP_n method derives from the $1D$ P_n equations extended in $3D$ by uncoupling the space directions and applying the $1D$ P_n system in each direction [6]. The SP_n equation system can be grouped two-by-two as pairs of even and odd equations, the even moments being scalar terms and the odd moments being vector terms *wrt.* the space variables. Thus, setting $\phi_{2k} = \varphi_h$ and $\boldsymbol{\phi}_{2k+1} = \boldsymbol{\psi}_h$ for $\forall 0 \le k, h \le (n-1)/2$, the SP_n system is written as [7]:

$$\frac{2h}{4h+1}\boldsymbol{\nabla}\cdot\boldsymbol{\psi}_{h-1}^g + \frac{2h+1}{4h+1}\boldsymbol{\nabla}\cdot\boldsymbol{\psi}_h^g + \sum_{g'=1}^{N_g}(\Sigma_t^g - \Sigma_{sl}^{g\to g'}\delta_{2h,l})\varphi_h^g = q_h^g,\ h = 0,2,4,\ldots,\frac{n-1}{2}$$

$$\frac{2h+1}{4h+3}\boldsymbol{\nabla}\varphi_h^g + \sum_{g'=1}^{N_g}(\Sigma_t^g - \Sigma_{sl}^{g\to g'}\delta_{2h+1,l})\boldsymbol{\psi}_h^g + \frac{2h+2}{4h+3}\boldsymbol{\nabla}\varphi_{h+1}^g = \boldsymbol{q}_h^g,\ h = 1,3,5,\ldots,\frac{n-1}{2}$$

with $\boldsymbol{\psi}_{-1} = \mathbf{0}$ and $\varphi_{(n+1)/2} = 0$.

Only, the first two flux moments have a physical meaning, the higher moments account for the higher flux harmonics which tend to decay quickly in reactor physics applications. The first SP_n equation is that for the zeroth flux moment. It is the balance equation that conserves the various reaction rates and power that are computed from the scalar flux. On the other hand, the higher moments correspond to higher flux harmonics which are of interest for anisotropic problems. The second equation for instance leads to the first flux moment, or the neutron current:

$$\boldsymbol{\psi}_1^g(\boldsymbol{r}) = \int_{4\pi}\mathrm{d}^2\mathbf{\Omega}\ \mathbf{\Omega}\phi^g(\mathbf{r},\mathbf{\Omega}) = \boldsymbol{j}(\boldsymbol{r})$$

This moment can be employed for energy collapsing in cases where the streaming effects are significant. Todorova *et. al.* [8] provided a simple method for approximating the first flux moment. Using such an approximation, two different total cross sections may be defined: one for even equations, and a second for odd ones.

3. First flux moment approximation

Let us consider the energy collapsing of the total cross section using an arbitrary function f^g as given by:

$$\Sigma_t^g(\boldsymbol{r}) = \sum_{g\in G}\Sigma_t^g(\mathbf{r})f^g(\mathbf{r}) \tag{6}$$

In the case where the total cross section is collapsed using the scalar flux, f^g is defined as:

$$f^g(\mathbf{r}) = \frac{\phi_0^g(\mathbf{r})}{\sum_{g\in G}\phi_0^g(\mathbf{r})} \tag{7}$$

If a current-collapsing is employed:

$$f^g(\mathbf{r}) = \frac{\|\boldsymbol{j}^g(\mathbf{r})\|}{\sum_{g\in G}\|\boldsymbol{j}^g(\mathbf{r})\|} \tag{8}$$

From the work [8], the authors assumed that the flux gradient has the same energy distribution as the scalar flux.

Hence, by using Fick's law approximation for the neutron current, the weighting function f^g can be expressed as follows to obtain an estimate for the first flux moment:

$$\begin{aligned} f^g(\mathbf{r}) &= \frac{\|\boldsymbol{j}^g(\mathbf{r})\|}{\sum_{g\in G}\|\boldsymbol{j}^g(\mathbf{r})\|} \\ &= \frac{\|D^g\boldsymbol{\nabla}\phi_0^g(\mathbf{r})\|}{\sum_{g\in G}\|D^g\boldsymbol{\nabla}\phi_0^g(\mathbf{r})\|} \\ &\sim \frac{D^g\phi_0^g(\mathbf{r})}{\sum_{g\in G}D^g\phi_0^g(\mathbf{r})} \\ &\sim \frac{\phi_1^g(\mathbf{r})}{\sum_{g\in G}\phi_1^g(\mathbf{r})} \end{aligned} \tag{9}$$

where we define the Todorova flux $\phi_1^g(\mathbf{r})$ as:

$$\phi_1^g(\mathbf{r}) = \frac{\phi_0^g(\mathbf{r})}{\Sigma_t^g(\mathbf{r}) - \sum_{g\in N_g}\Sigma_{s1}^{g'\to g}(\mathbf{r})} \tag{10}$$

Thus, the total cross section can be collapsed using an approximation of the first flux moment, the Todorova flux, instead of the scalar flux as was discussed previously:

$$\Sigma_t^G(\mathbf{r}) = \frac{\sum_{g\in G}\Sigma_t^g(\mathbf{r})\phi_1^g(\mathbf{r})}{\sum_{g\in G}\phi_1^g(\mathbf{r})} \tag{11}$$

$$\Sigma_{sl}^{G'\to G}(\mathbf{r}) = \frac{\sum_{g'\in G'}\sum_{g\in G}\Sigma_{sl}^{g'\to g}(\mathbf{r})\phi_1^{g'}(\mathbf{r})}{\sum_{g'\in G'}\phi_1^{g'}(\mathbf{r})}, \text{ if } l \text{ is odd.} \tag{12}$$

However, these *Todorova-collapsed* cross sections are applied only in the odd SP_n equations with those for the even equations being condensed in energy using the usual scalar flux. Thus, the neutron balance is conserved through the zeroth flux moment while only higher harmonics are impacted to allow for spectral effects.

III. METHOD VALIDATION

In this section, the energy-collapsing method for the odd total cross sections and the odd-moment differential scattering cross sections are tested using two cases:

- an elementary 3×3 colorset is employed as in [3]
- the KAIST 1A benchmark.

The cross section library for the Cocagne code are generated for various energy-group structures (ranging from 2 to 26) with the Apollo2-REL2005 scheme. The Todorova flux is computed from the 26-group cross section library using the scalar flux, the total and the P_1 scattering cross sections in each computational region. It is then used to collapse the total cross section (*odd total*) and the odd differential scattering moments for the various multigroup libraries. These cross sections are injected in the SP_n solver of Cocagne.

Therefore, the multigroup SP_3 calculations are carried out using P_1 and P_3 (all cross sections collapsed with the scalar flux) or *Todorova*-P_1 (TP_1) and *Todorova*-P_3 (TP_3) (total cross sections for the odd equations and odd scattering moments are collapsed with the Todorova flux) for 4, 6, and 8 energy groups (which are derived from the 26 group structure) for the above configurations.

1. Equivalence factors

The various calculations for this work are carried out for pin-homogenised cross sections. Unlike assembly-homogenised core calculations, this implies that we must apply some equivalence factor at the boundaries of the assembly to ensure that the reaction rates for the homogenized and condensed cross sections conserve the reaction rates from the assembly calculations [9].

The formalism used in COCAGNE is called the SPH (*SuPerHomogenisation*) method. The latter defines equivalence factors for each cell m of the computational mesh and each energy group g. Besides, the equivalence factor also depends on the transport operator and thus also on the anisotropy of the problem. Hence, for each anisotropy, similar to classical scalar-flux-condensed cross sections, equivalence factors for Todorova-condensed cross sections are also defined and computed. These factors will be applied to the corresponding cross sections for all calculations.

Thus, this step ensures that core calculations are carried out in the same conditions for all configurations studied.

2. Assembly colorset

The 3×3 colorset studied includes a fresh central MOX-1 assembly surrounded by UOX-2 assemblies at 24 GWd/ton burn-up (the assemblies are taken from the KAIST benchmark which will be described later). The goal of using this colorset is to evaluate the use of the energy-collapsing strategy on a simple UOX-MOX interface where pins are subjected to a high flux gradient (different neutronic properties due to material composition).

The best-estimate calculation is a 26 group $SP_3 - P_3$ calculation with pin-homogenized cross sections in the Cocagne platform. The reference k_{eff} value is 1.11638. For each anisotropy previously described, calculations are carried out with the SP_3 solver for 4, 6 and 8 groups and the results are compared to the best-estimate results for reactivity and local pin values.

Figure 1 shows that the discrepancies at the UOX-MOX interfaces are reduced using TP_3 since the TP_3 cross sections are collapsed with a weighting function that allows for harder spectral variations. From the results in Table I, it is interesting to note that:

- As the number of groups is increased, there is sufficient

Groups	Anisotropy	$\Delta k_{eff}(pcm)$	min. (%)	max. (%)	rms. (%)
4	P_1	-121	-3.4	3.5	0.9
4	P_3	-121	-3.5	3.6	0.9
4	TP_1	-105	-2.2	2.5	0.5
4	TP_3	-104	-2.2	2.6	0.5
6	P_1	-70	-2.7	1.7	0.5
6	P_3	-68	-2.8	1.8	0.5
6	TP_1	-66	-2.4	0.9	0.3
6	TP_3	-65	-2.4	1.0	0.3
8	P_1	-56	-2.6	1.0	0.4
8	P_3	-55	-2.6	1.1	0.4
8	TP_1	-54	-2.2	0.4	0.3
8	TP_3	-52	-2.2	0.5	0.3

TABLE I: Reactivity and local pin power discrepancy results on the assembly colorset.

spectral data to obtain satisfactory results on integral quantities such as the reactivity, and thus the TP_n cross sections leads to the same results as the P_n ones.

- On the other hand, the local pin power is a more heterogeneous information as it is a local quantity and is more subject to spectrum effects. Thus, if the number of groups is not sufficient, the P_n cross sections are less accurate and lead to higher discrepancies on the local pin power. Using the Todorova-collapsed cross sections, it can be observed that the results for the 4-group calculation is as good as that for P_n results at 6 groups, and the same conclusions can be drawn for the 6-group TP_n compared to the 8-group P_n results. Furthermore, the discrepancy spreads are always much lower with TP_n method.

3. KAIST 1A benchmark problem

This benchmark problem has been published by N. Cho[4]. The KAIST 1A benchmark is a small MOX-loaded core, basically a simplified PWR problem of reduced size (hence power) and consists of 52 assemblies producing 900 MWth at nominal power. Figure 2 shows a description of the radial map of those assemblies in the core at zero burn-up.

The core contains five types of assemblies:

- UOX-1: UOX assembly enriched at 2.0% ^{235}U,
- UOX-2: UOX assembly enriched at 3.3% ^{235}U, with BA-16, it implies that there are 16 gadolinia pins,
- MOX-1: MOX assembly with zoning for plutonium enrichment: 8.7% enrichment in the central zone, 7.0% in in the intermediate zone and 4.3% in the peripheral zone, with BA-8, there are 8 gadolinia pins.

The gadolinia pins are enriched in gadolinium isotopes at 9.0% on natural uranium support. CR refers to the rodded configuration of the core where all the guide tubes, except the central one, are filled with B_4C rods. The core is enclosed by a stainless steel baffle. The reflector is simple and consists of water at 570K and has the same composition as the moderator with 800 ppm of soluble boron concentration.

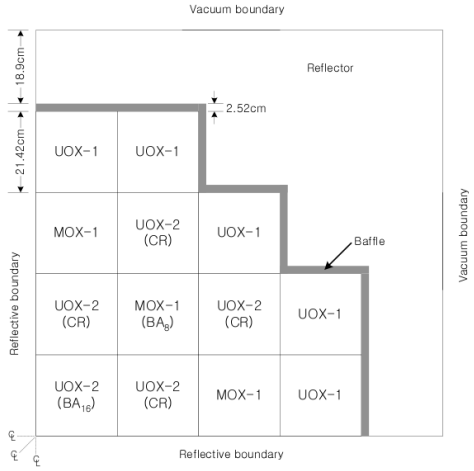

Fig. 2: The KAIST 1A core with its assemblies.

KAIST 1A offers a very interesting study case as it is in 2D and temperatures are imposed in the benchmark problem. In the case of the validation of the Todorova-flux method, the KAIST 1A benchmark offers a very challenging case with a small but highly heterogeneous core with both UOX-MOX and core-reflector interfaces. This core can be depleted for numerical validation purposes without imposing any thermal-hydraulics which significantly complexifies the analysis.

The Todorova flux is employed for energy collapsing of cross sections for both fuel and reflector assemblies. The best-estimate calculation is a 26-group $SP_3 - P_3$ calculation with pin-homogenized cross sections in the Cocagne platform. All the calculations for all the energy groups and anisotropy orders are carried out using the pin-homogenised cross sections. The reference k_{eff} value is 1.13257. For each anisotropy previously described, calculations are carried out with the SP_3 solver for 4, 6 and 8 groups and the results are compared to the

Fig. 1: Pin power comparisons between the 4-group SP_3 with P_3 (left) and TP_3 (right) and the best-estimate calculations.

best-estimate results for reactivity and local pin values.

A. Results for zero-burnup calculations

The results for step zero (zero burnup) calculations are given in Figure 3 and Table II. From Table II, it can be observed that the new collapsing method leads to larger discrepancies in reactivity. Besides, there is a change in the sign of the discrepancy and thus, where the scalar-flux collapse leads to overestimation, the new method leads to an underestimation of the k_{eff}. This effect was not observed on the assembly clusters studied in the previous section. Hence, it can be deduced that the Todorova collapsing method impacts the reflector effects. Therefore, it is incumbent to analyse reaction rates to ensure that there are no compensation effects.

From Table II, it can be observed that the Todorova-condensed cross sections decrease the dispersion between the minimum and maximum discrepancies. This is translated on Figure 3 as a better prediction of the pin power distribution since the in-out shift is less visible for the lower ones. Hence, it can be deduced that the Todorova-collapsed cross sections lead to better spectral distribution of neutrons and thus, power maps. For the scalar-flux collapsing method (figures in the upper row), it can be seen that the power distribution is biased by an in-out shift which thus leads to compensation effects on the global core reactivity. Such effects are not observed with the new method and the power distributions are very smooth, without trends from the inside of the core to its periphery.

Furthermore, it can also be observed that the RMS value of the discrepancies decreases for the TP_n cross sections. The same conclusions that were observed for the assembly clusters can be extrapolated for the core calculations. For this benchmark, it is very encouraging to obtain 4-group results that are almost of same quality as 6-group ones (even slightly better) and are below 1%, which is highly satisfactory for industrial uses.

B. Depletion calculation results

Following the work on zero burnup calculation, the next step is to test the collapsing method on depletion calculations. In [3], the KAIST 1A core has been depleted using different solvers and simulations, with a 1D reflector model [10]. From this work, we observed that two-group diffusion calculations were much better than multigroup SP_3 calculations if the number of groups were not sufficient. Thus, we concluded that simplified transport required sufficient number of groups to allow for spectral effects, especially for such a small heterogeneous core.

Following this observation, the Todorova-collapsed cross section libraries were used for depletion of the KAIST 1A benchmark with the same simulation as the previous paper. Isotopic depletion computations were carried out on the KAIST 1A core and the boron concentration c_B was computed at each step. No thermalhydraulics feedback was employed for these computations to compare only the collapsing effect, without any additional bias. Our aim is to verify whether the previous observation for static zero burnup calculations holds true even during depletion. For this simulation, we have also added pin-by-pin two-group diffusion calculation, which is a coarser approximation.

Figure 4 shows the discrepancy on the critical boron concentration for 4, 6 and 8 energy groups against an $SP_3 - P_3$ reference calculations for both condensation models. It can be observed that there are two sets of plots, those for the scalar flux and those for the Todorova-condensed cross sections. The first set corresponds to the same observations as that in [3] whereby the diffusion calculation leads to more satisfactory results than multigroup SP_3. Indeed, the spectral effects on the condensation of cross sections to few energy groups leads to significant discrepancies when applied to this benchmark. Diffusion, on the other hand, is a much better approximation leading to widely acceptable results. For the TP_n cross sections, there is a change in the sign of the observed discrepancies as well as a decrease in their magnitude. Furthermore, the discrepancies remain more or less stable over the depletion process.

Table III shows the RMS discrepancies for pin power distributions at beginning, middle and end of cycle (BOC, MOC and EOC). The same tendency can be observed over the cycle for the pin power discrepancies. As the number of groups increases, the condensation effects are less significant. Nonetheless, the discrepancies are more stable over the cycle for the Todorova-collapsed cross sections.

Groups	Anisotropy	$\Delta k_{eff}(pcm)$	min. (%)	max. (%)	rms. (%)
4	P_1	109	-4.8	4.2	1.6
4	P_3	120	-4.7	4.2	1.6
4	TP_1	-211	-2.3	3.8	0.9
4	TP_3	-200	-2.4	3.9	0.9
6	P_1	112	-3.9	2.4	1.0
6	P_3	123	-3.9	2.3	1.1
6	TP_1	-199	-2.1	1.8	0.6
6	TP_3	-186	-2.1	1.8	0.5
8	P_1	111	-3.4	1.7	1.0
8	P_3	122	-3.4	1.6	0.9
8	TP_1	-197	-1.7	2.3	0.4
8	TP_3	-185	-1.7	2.0	0.4

TABLE II: Reactivity and local pin power discrepancies for the KAIST 1A benchmark problem at zero burnup.

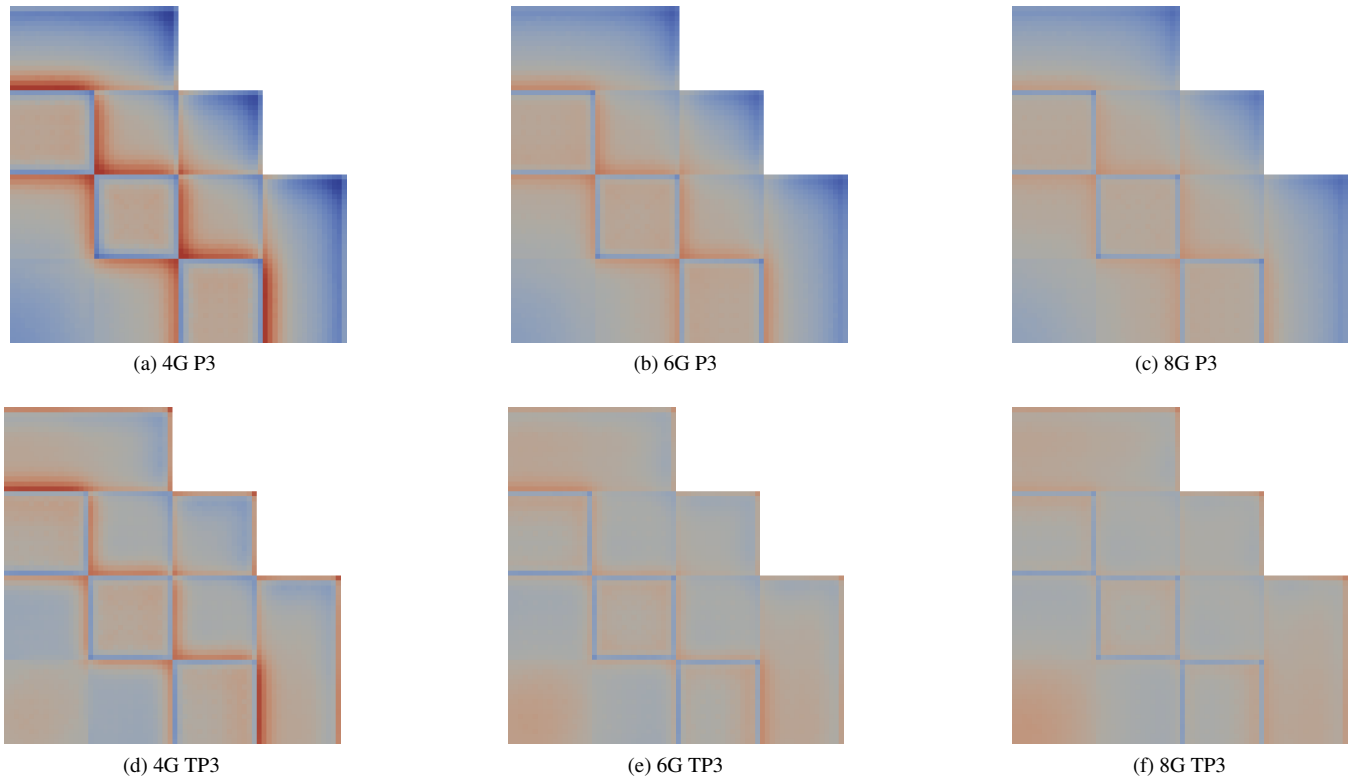

(a) 4G P3 (b) 6G P3 (c) 8G P3

(d) 4G TP3 (e) 6G TP3 (f) 8G TP3

Fig. 3: Local pin power discrepancies for the KAIST 1A benchmark problem at zero burnup. All figures are scales to -5 – 5%. Figures on the top row correspond to the comparison of computations with “usual” scalar-flux-collapsed cross sections. On the other hand, the bottom row shows results for Todorova-collapsed cross sections.

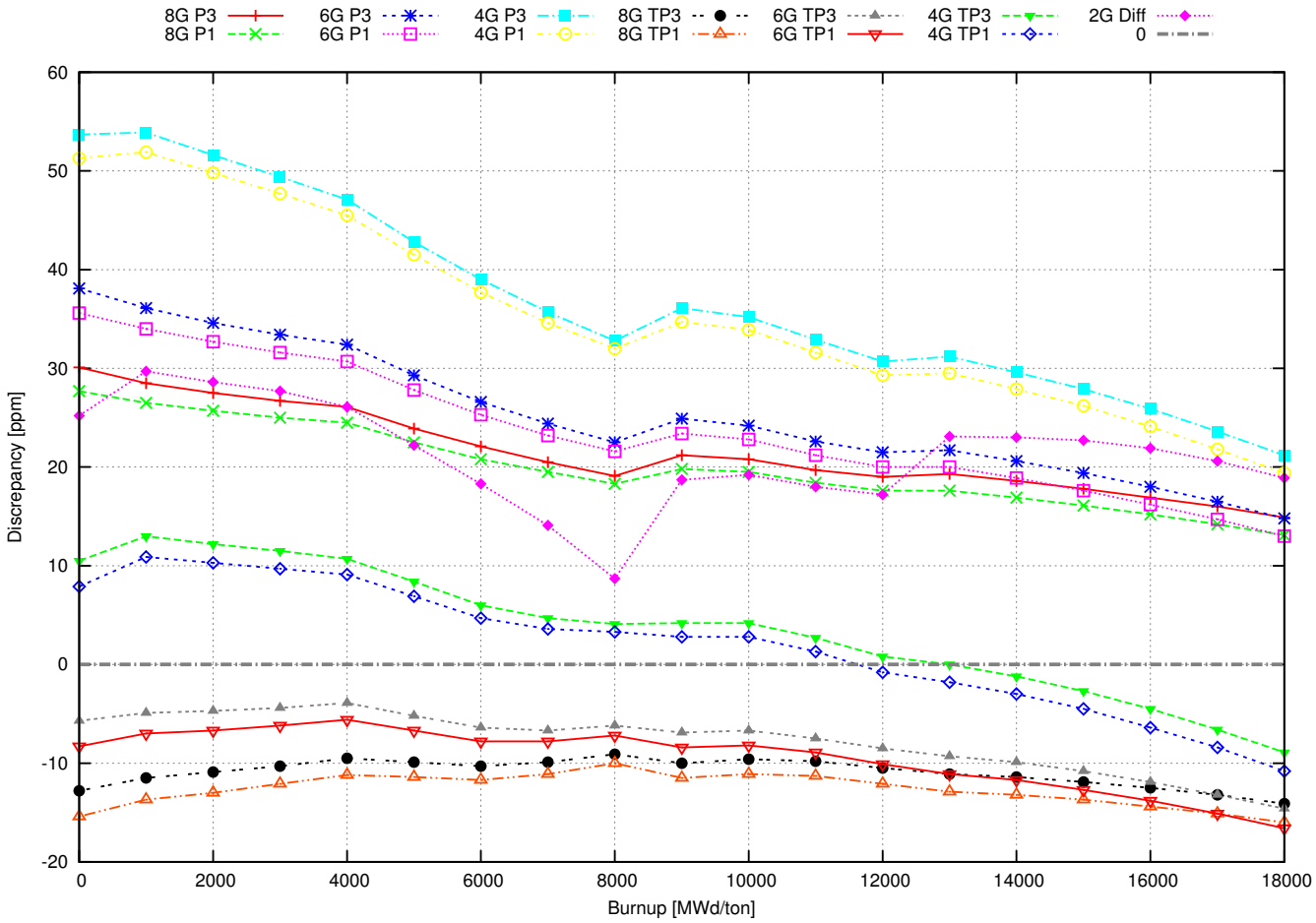

Fig. 4: Discrepancy on the critical boron concentration for 4, 6 and 8 energy groups against a 26-group $SP_3 - P_3$ reference calculations for both condensation models.

Groups	Anisotropy	BOC (%)	MOC (%)	EOC (%)
4	P_1	2.0	1.4	1.3
4	P_3	2.1	1.5	1.3
4	TP_1	0.9	0.8	0.7
4	TP_3	0.9	0.8	0.7
6	P_1	1.5	1.0	0.9
6	P_3	1.6	1.0	0.9
6	TP_1	0.5	0.5	0.6
6	TP_3	0.5	0.5	0.5
8	P_1	1.2	0.9	0.7
8	P_3	1.3	0.9	0.8
8	TP_1	0.5	0.4	0.5
8	TP_3	0.4	0.4	0.5

TABLE III: RMS local pin power discrepancies for the KAIST 1A benchmark problem at BOC, MOC and EOC.

IV. CONCLUSIONS

In this work, the goal was to apply a simple method to evaluate a more convenient energy-collapsing method for heterogeneous spectral problems with few energy groups in the SP_n framework within the COCAGNE platform. The Todorova flux was successfully applied as a satisfactory approximation for the neutron current or first flux moment to collapse the cross sections which are injected in the odd equations of the SP_n equation system.

Two cases were studied to validate the method, an assembly colorset and the KAIST 1A benchmark. The results on the assembly colorset were satisfactory both for integral and local quantities for a UOX-MOX interface. Results on the KAIST 1A benchmark for eigenvalue calculations as well as depletion calculations are very encouraging. The discrepancies on reactivity are slightly worsened but remain within an acceptable range. Yet, the most important aspect is the fact that pin-power discrepancies are improved both in magnitude and in their distribution - there is no in-out shift on the core.

The claim is that despite the widespread beliefs that the SP_n method works only if sufficient energy groups are employed, it is shown that a more adapted energy-collapsing method may be applied to obtain satisfactory results with few energy groups.

V. ACKNOWLEDGMENTS

The authors acknowledge the wise advice of Pr. Alain Hébert from École Polytechnique de Montréal on the subject matter.

REFERENCES

1. HEBERT, A., *Applied Reactor Physics*, Presses Internationales Polytechnique (2009).
2. CALLOO, A., LEROYER, H., FLISCOUNAKIS, M., COUYRAS, D., "Core Neutronics Methodologies Applied to the MOX-loaded KAIST 1A benchmark: reference to industrial calculations," in "Proceedings of PHYSOR 2014," The Westin Miyako, Kyoto, Japan (October 2014).
3. CALLOO, A., HUY, S., COUYRAS, D., BROSSELARD, C., FLISCOUNAKIS, M., "Validation of the SP_n depletion schemes of the EDF GABV2-COCAGNE tools using the KAIST 1A benchmark," in "Proceedings of PHYSOR 2016," Sun Valley, Idaho, USA (May 2016).
4. CHO, N. Z., "KAIST Nuclear Reactor Analysis and Particle Transport Laboratory, *Benchmark Problem 1A*," http://nurapt.kaist.ac.kr/benchmark.
5. VIDAL, J.-F., ARCHIER, P., CALLOO, A., JACQUET, P., TOMMASI, J., LE TELLIER, R., "An Improved Energy-Collapsing Method for Core-Reflector Modelization in SFR Core Calculations using the PARIS platform," in "Proceedings of PHYSOR 2012," Knoxville, Tennessee, USA (April 2012).
6. LARSEN, E., MOREL, J., MCGHEE, J., "Asymptotic derivation of the multigroup P_1 and simplified P_n equations with anisotropic scattering," *Nuclear Science and Engineering*, **123**, *123*, 328–342 (2008).
7. HAMILTON, S. P., EVANS, T., "Efficient solution of the simplified P_n equations," *Journal of Computational Physics*, **284**, *C*, 155–170 (2015).
8. TODOROVA, G., NISHI, H., ISHIBASHI, J., "Method for Condensation of the Macroscopic Transport Cross Sections for Criticality Analyses of FBR MONJU by the code NSHEX," *Journal of Nuclear Science and Technology*, **41**, *12*, 1237–1241 (2004).
9. CALLOO, A., COUYRAS, D., FÉVOTTE, F., GUILLO, M., "COCAGNE: EDF new neutronic core code for ANDROMEDE calculation chain," in "Proceedings of *this conference*," Jeju, Korea (2017).
10. HUY, S., GUILLO, M., CALLOO, A., BROSSELARD, C., COUYRAS, D., "Multigroup 1D-Reflector Modelling for EDF PWR," in "Proceedings of PHYSOR 2016," Sun Valley, Idaho, USA (May 2016).